http://dx.doi.org/10.5935/0103-5053.20160072

J. Braz. Chem. Soc., Vol. 27, No. 10, 1866-1871, 2016.
Printed in Brazil - ©2016 Sociedade Brasileira de Química
0103 - 5053 $6.00+0.00

Article

Tunable Photochemical/Redox Properties of (Phenylthio)$_n$corannulenes: Application to a Photovoltaic Device

Angela Steinauer,[a] Anna M. Butterfield,[a] Anthony Linden,[a] Agustin Molina-Ontario,[b] David C. Buck,[b] Robert W. Cotta,[b] Luis Echegoyen,[b] Kim K. Baldridge[,a,c] and Jay S. Siegel*[,a,c]*

[a]*Department of Chemistry, University of Zurich, 8057 Zurich, Switzerland*

[b]*Department of Chemistry, University of Texas at El Paso, 79968 El Paso-TX, USA*

[c]*School of Pharmaceutical Science and Technology, Tianjin University, 300072 Nankai District-TJ, China*

The additive substituent effect of phenylmercapto derivatives of corannulene are investigated by spectroscopic, electrochemical, and computational techniques. The per-substituted phenylmercaptocorannulene is incorporated as a replacement for [6,6]-phenyl-C_{61}-butyric acid methyl ester (PCBM) in a photovoltaic device.

Keywords: photovoltaic, electrochemistry, corannulene, photochemistry

Introduction

In a similar fashion to fullerenes,[1] curved aromatic hydrocarbons, like corannulene, **1**, behave as electron-deficient π-systems,[2] the redox properties of which can be tuned by derivatization (Figure 1).[3] Curved aromatic hydrocarbons related to corannulene have been used in various materials applications including the development of fluorescent chemosensors,[4] organic field-effect transistors,[5] and heterojunction photovoltaics.[6] In each case, specific photochemical and redox properties have been important to the success of the application. Tuning the photochemical and redox properties of corannulene cognates corresponds to influencing the highest occupied molecular orbital (HOMO) and lowest unoccupied molecular orbital (LUMO) levels as well as the HOMO-LUMO gap. Whereas simple alkyl substituents raise HOMO and LUMO levels,[7] fluorinated alkyl groups lower both;[8] in neither case is there a substantial effect on the HOMO-LUMO gap as gauged from absorption spectroscopy. Organothio-substituents raise HOMO and lower LUMO levels such that one can obtain good electron acceptors with smaller HOMO-LUMO gaps.[9] For example, compared to **1**, a pale yellow material with first reduction at −2.33 eV in acetonitrile, decasubstitution of **1** with thiophenol (SPh) produces a deep red material with the first reduction potential at −1.22 eV,[10] which is similar to the reported value of −1.17 volts for [6,6]-phenyl-C_{61}-butyric acid methyl ester (PCBM). Given that many high-performing organic photovoltaic (OPV) devices rely on C_{60} and its derivatives to act as electron acceptors,[11] this similarity in electrochemistry between PCBM and decakisphenylmercaptocorannulene motivates a study into the nature of tuning the physical properties (electrochemistry, ultraviolet-visible (UV-Vis) absorption, fluorescence, and phosphorescence) of corannulene by phenylmercapto substitution and the photovoltaic characterization of decakis(phenylthio-)corannulene as an acceptor in an OPV device. Furthermore, the optoelectronic tunability of corannulenes makes them potentially useful as organic light emitting diodes (OLEDs),[12] as organic conductors,[13] or in high density carbon electrodes.[14]

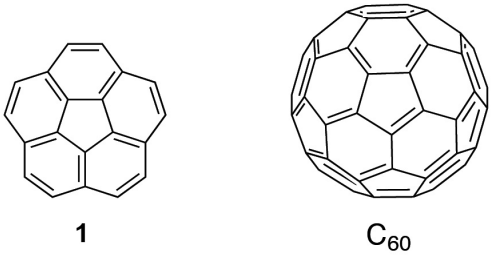

Figure 1. Corannulene and C_{60}.

*e-mail: kimb@tju.edu.cn; dean_spst@tju.edu.cn

Experimental

General synthesis

1,3-Dimethyl-2-imidazolidinone (DMI; 5-10 mL, dried over molecular sieve) was added to a round bottom flask equipped with a reflux condenser. Thiophenol (1.5 equiv./reaction site) and sodium hydride (1.2 equiv./reaction site, 60% in mineral oil) were added and stirred at room temperature for 10 min. The halogenated corannulene derivative (**2a**-**7a**, 1 equiv.) was added and the solution was heated at 60 °C for 18 h. The solution was cooled and extracted three times with dichloromethane (DCM; 15-20 mL). The combined organic layers were washed with water, dried over magnesium sulfate, filtered, and the solvents were removed under reduced pressure. The product was purified by column chromatography (silica gel) with a hexane/DCM mixture as eluent (0-25% DCM, depending on the compound). Compound **5b** was further purified by high-performance liquid chromatography (HPLC). The yield of a light yellow to dark red solid (**2b**-**7c**) was 28-89%. Further experimental details can be viewed in the Supplementary Information.

Computational methods

The conformational analyses of the molecular systems described in this study, including structural and orbital arrangements, were carried out with the dispersion-enabled functional, B97-D,[15] using an ultrafine grid for evaluation of integrals together with the def2-TZVPP basis set.[16] Full geometry optimizations were performed and uniquely characterized via second derivatives (Hessian) analysis to determine the number of imaginary frequencies (0 = minimum; 1 = transition state) as well as zero point and thermal corrections. Effects of solvation were taken into account with the COSab method,[17] using the dielectric for tetrahydrofuran (THF) and solvent radii from Klamt *et al.*[18] Ionization potentials were determined using ΔSCF/CBS-4M[19]//B97D/Def2-TZVPP. Reduction potentials were determined using $E° = -\Delta G/nF$, where n = 1, and F = 1 eV, corrected to the Ag/AgCl electrode (4.52 eV). Molecular orbital contour plots, used as an aid in the analysis of results, were generated and depicted using the program Avogadro.[20]

Results and Discussion

Synthesis

Halogenated corannulenes, **2a**-**7a** were synthesized according to literature procedures (the reference for **2a** and **7a** is 21; and for **3a**, **5a**, **6a** and **4a** are 7, 22, 23 and 24, respectively). Conversion to *n*-phenylthiocorannulenes, **2b**-**7b**, was performed via direct nucleophilic substitution using sodium hydride as a base and SPh as the pro-nucleophile (Scheme 1). Alternatively, substitution with cyclohexanethiol or methylX could be performed to yield **7b*** and **3c**-**7c**,[7] respectively.

X-Ray crystallography

Pentakis(phenylthio)-corannulene (**6b**) was crystallized in DCM/hexane (monoclinic $P2_1/n$). In contrast to **1**, **6b** displays pairwise bowl-in-bowl aggregation in its crystal packing with two molecules in the asymmetric unit (Figure 2). In one molecule, all substituents lie below the rim of the corannulene bowl, whereas in the other molecule, three substituents are oriented above the rim. The bowl

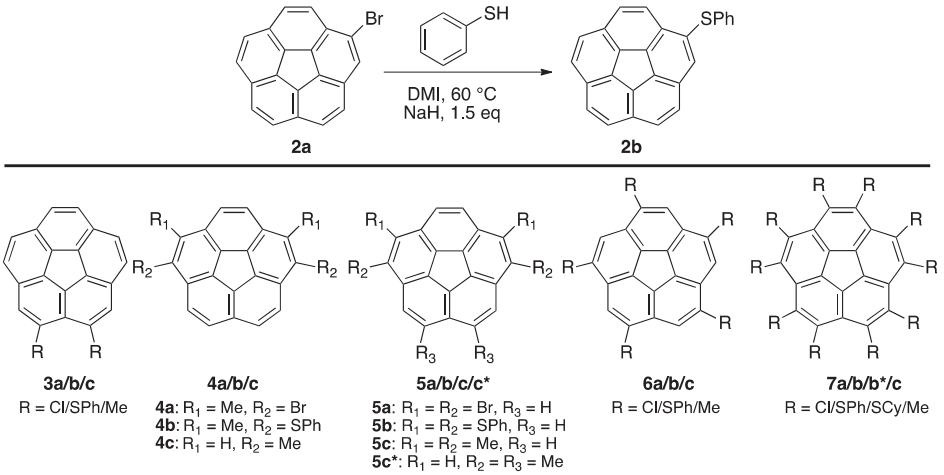

Scheme 1. Synthesis of corannulenes **2b**-**7c** from **2a**-**7a**. Above: representative reaction scheme for **2a** to **2b**; below: substitution pattern and substituent identity for starting materials and products in the series **3**-**7**. DMI: 1,3-Dimethyl-2-imidazolidinone; Me: methyl; NaH: sodium hydride; SCy: mercaptocyclohexyl; SH: thiol; SPh: mercaptophenyl.

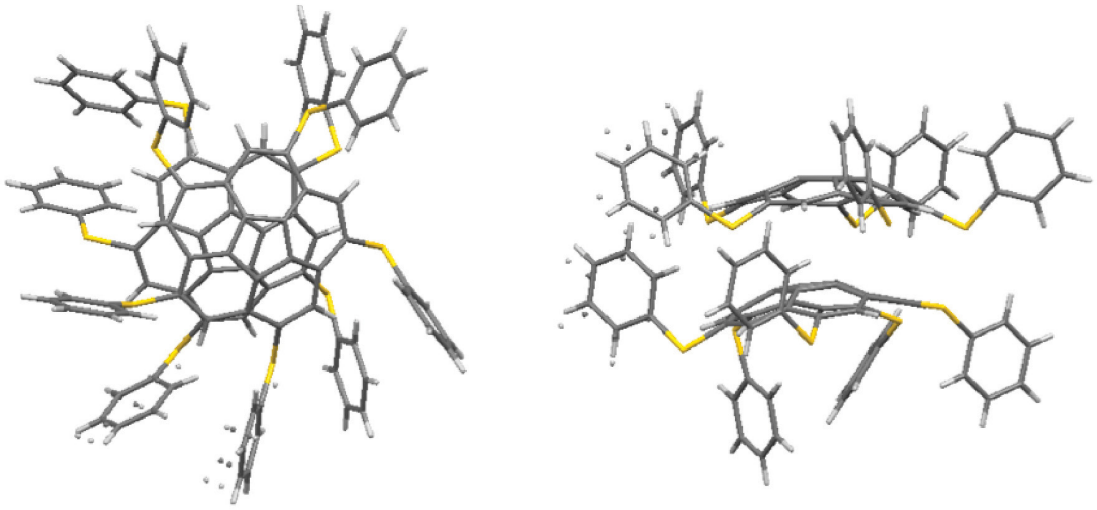

Figure 2. Molecular structure of the two independent molecules of **6b** from X-ray diffraction analysis. Top and side views.

depths (hub-to-rim) in the two molecules of **6b** are 0.866 and 0.908 Å, respectively, which is close to the bowl depth of **1** (0.87 Å).[25] In **7b,** with ten substituents, five above and five below the rim, the steric demands flatten the bowl considerably (0.486 Å).[10]

Photophysical and redox properties

The UV-Vis absorption spectra of **2b**-**7b** and **7c** are shown in Figure 3. Each SPh addition shifts the longest wavelength absorption [λ(2)] bathochromically 10-15 nm while leaving the maximum absorption wavelength [λ(1)] relatively unshifted (Table 1). The linearity of the bathochromic shift is shown in the inset of Figure 3. This shift results in a change from colorless **1** to orange-red **7b** (Figure 4). These data suggest a diminution of the HOMO-LUMO gap.

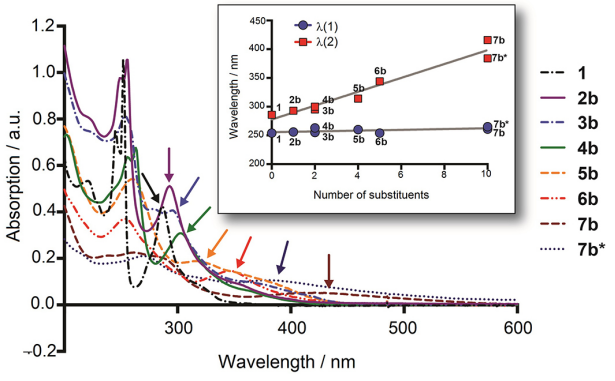

Figure 3. Ultraviolet visible (UV-Vis) spectra of thiophenol (SPh)$_n$-corannulenes **2b**-**7b**. Inset: λ(1) and λ(2) correlated with the number of SPh substituents (measuring conditions as in Table 1).

This is also evidenced by the difference in reduction and oxidation potentials (Table 2). For **7b,** the reduction

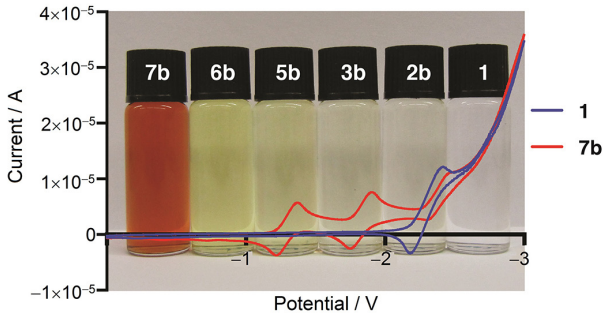

Figure 4. Graph: cyclic voltammetric curves of **1** and **7b** (conditions cf. Table 2). Background image: solutions of **1**, **2b**, **3b, 5b**-**7b** in dichloromethane (DCM) at 500 μmol L^{-1}.

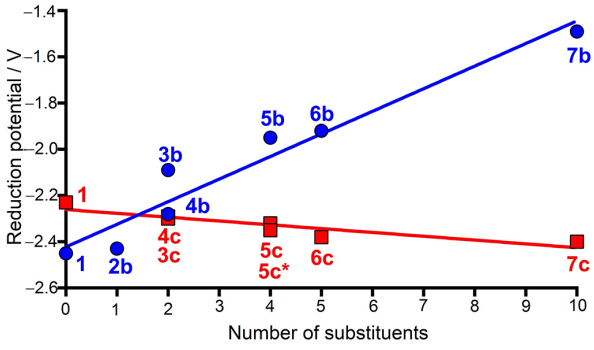

Figure 5. Correlation of reduction potentials of compounds **1, 2b**-**7b** (tetrahydrofuran, THF; circle) and **1, 3c**-**7c** (acetonitrile; square) *vs.* number of substituents (conditions cf. Table 2).[7]

and oxidation potentials are each ca. 1 eV easier to achieve than for **1** (D_{redox} **7b** = 2.05 eV *vs.* D_{redox} **1** = 4.02 eV). Linear regression of the first reduction potential *vs.* the number of SPh groups suggests a stabilization effect of the radical anion by ca. +0.1 V/SPh group (Figure 5). The opposite trend is seen for the methyl series **1**-**7c** (ca. –0.02 V).

Although oxidations were largely irreversible, except for **7b**, a crude estimation of the ionization potentials was possible from the oxidation waves by using Cavalieri's method (Table 2).[26] Whereas isolated SPh groups provide small stabilization of the radical cation, as in **6b** *vs.* **1**, *peri*-substitution provides a substantial stabilization effect, as in **3b**.

Emission spectra also shift to longer wavelengths with increasing SPh-substitution of **1** (Table 1). Fluorescence quantum yields from 1 up to 20% were observed and lifetimes were between 1-10 ns across the series and can be seen in Figure 6. The difference between the longest absorption and shortest emission ranges from 50-70 nm suggesting little structural change in the fluorescent state. At 77 K, phosphorescence can be observed at about 100-120 nm longer wavelength than the fluorescent emission. Again, higher substitution leads to longer wavelength phosphorescence. Understanding this behavior may be a key to the development of cognates as photonic materials.

Charge-transfer absorptions between tetracyanoethylene (TCNE) and the $(SPh)_n$ series were measured using the Kuroda method in order to deduce ionization potential (IP) values.[29] Weak charge-transfer (CT) bands appear at 512-632 nm; however, the spectra are not precise enough to calculate useful IP values from CT absorptions (IP_{CT}). In the case of **7**•TCNE, no CT band was observed, which may be due to the increased steric hindrance. In general, steric hindrance of the π system in these systems may preclude the use of a classical CT band to IP correlation model; the

Table 1. Photophysical properties of **1**-**7b, 7b***

Compound	λ_a / nm (log ε [M^{-1} cm^{-1}])	λ_f / nm	$\lambda_s = \lambda_f - \lambda_a$ / nm	Φ_f	[ns]	λ_p / nm
1	196 (4.9), 221 (4.7), 252 (λ_{max}) (4.9), 286 (λ_{exc}) (4.6)	348, 422 (λ_{max})	62	0.04	10.0	483, 515 (λ_{max}), 553, 598
2b	194 (4.7), 250 (4.7), 255 (λ_{max}) (4.7), 292 (λ_{exc}) (4.4)	356, 448 (λ_{max})	64	0.05	1.1	566 (λ_{max})
3b	254 (λ_{max}) (4.6), 278 (4.3), 295 (λ_{exc}) (4.3)	365, 456 (λ_{max})	70	0.04	5.6	535, 559 (λ_{max})
4b	200 (4.8), 256 (4.8), 263 (λ_{max}) (4.8), 302 (λ_{exc}) (4.4)	354, 460 (λ_{max})	52	0.20	1.5	565 (λ_{max})
5b	260 (λ_{max}) (4.8), 310 (λ_{exc}) (4.3)	380, 496 (λ_{max})	70	0.02	1.7	555, 604 (λ_{max}), 652
6b	252 (λ_{max}) (4.9), 344 (λ_{exc}) (4.5)	405, 492 (λ_{max})	61	0.01	0.8	560, 600 (λ_{max}), 645
7b	235 (5.0), 260 (λ_{max}) (5.0), 417 (λ_{exc}) (4.4)	–	–	0.00	–	725 (λ_{max})
7b*	265 (λ_{max}) (3.9), 316 (3.8), 384 (λ_{exc})(3.7)	433 (λ_{max}), 531	49	0.01	6.0	728 (λ_{max})

Measurement (solvent): phosphorescence (2-methyltetrahydofuran, MeTHF); absorption and fluorescence (acetonitrile). Quantum yields (Φ_f): **1**-**5b** relative to 2,5-diphenyloxazole (PPO, $\Phi_f = 0.94$) in cyclohexane; **6b** and **7b**-**c** relative to 10-(3-sulfopropyl)acridinium betaine (SPA, $\Phi_f = 0.57$) in water. λ_a: $\lambda_{absorption}$; λ_{exc}: $\lambda_{excitation}$; λ_f; $\lambda_{emission}$; λ_{max}: $\lambda_{maximum\ wavelength\ of\ absorption}$; λ_p: $\lambda_{wavelength\ of\ phosphorescence}$; λ_s: $\lambda_{Stokes\ Shift}$; [ns]: fluorescence lifetime.

Table 2. Reduction potentials (Red_{CV}), oxidation potentials (Ox_{CV}) and ionization potentials (IP_{CV}) of **1**, **2b**-**7c**

Compound	Red_{CV}[a] / V	Ox_{CV} / V	IP_{CV} / eV	ΔIP / eV
1	–2.45 [–2.49][b]	+1.57[irrev,2,27]	7.96 [7.92][c]	0.41
2b	–2.43 [–2.34][b]	+1.25-1.35[irrev]	7.33 [7.64][c]	0.67
3b	–2.09 [–2.15][b]	+1.05-1.15[irrev]	7.11 [7.38][c]	0.41
4b	–2.28 [–2.17, –2.22, –2.12][b,d]	+1.15-1.25[irrev]	7.68 [7.77, 7.18, 7.75][c,d]	–
5b	–1.95 [–1.85][b]	+1.35-1.45[irrev]	7.73 [8.28][c]	0.37
6b	–1.92 [–2.02, –1.90],[b,d] –2.53	+1.4-1.5[irrev]	7.64	0.36
7b	–1.49 [–1.55],[b] –2.02, –2.58	+0.6-0.7	6.25	–
7b*	–2.00, –2.74	+1.1-1.2[irrev]	7.24	–

[a]Cyclic voltammetry: 1 mmol L^{-1} compound **1**-**7b*** and 0.07 mol L^{-1} tetrabutylammonium hexafluorophosphate ($TBAPF_6$) in tetrahydrofuran (THF; 298 K). Electrodes: working, glassy carbon; reference, Ag/Ag^+ in acetonitrile (ACN); counter, platinum wire. Scan rate = 0.1 V s^{-1}. All $E_{1/2}$ potentials are direct averages of the cathodic and anodic peak potentials. Internal standard: ferrocinium/ferrocene couple (+0.085 V for THF);[27] [b]Values in brackets are B97D/Def2-TZVPP(THF) $E° = -\Delta G/nF + E_{ref}$, n = 1, F = 1 eV, corrected to Ag/AgCl electrode, 4.52; [c]ΔSCF/CBS-4M IP; [d]for **4b** and **6b** values are ranked in accordance with the relative energy ordering of the isomers. irrev: irreversible.

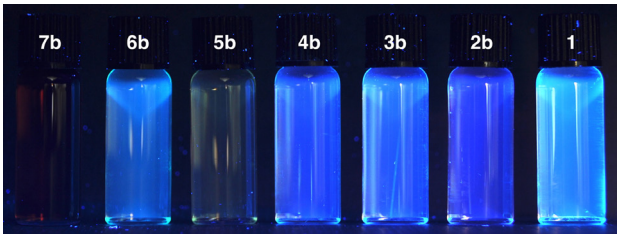

Figure 6. Fluorescence of **1**-**7b** in dichloromethane (DCM) at 500 μmol L^{-1} (illumination at 360 nm).

change in the geometry of the complex having a greater effect than the change in electronic π character.

Photovoltaic device performance

Because the reduction potentials are close to those of active fullerene derivatives, **7b** was chosen to test the acceptor capabilities of these compounds in organic photovoltaic devices. The results are shown in Figure 7, and the cell parameters are summarized in Table 3. The best power conversion efficiency (PCE) of 0.30% was achieved by an active layer of 3:2 **7b**:poly-(3-hexylthiophene) (P3HT) by mass.

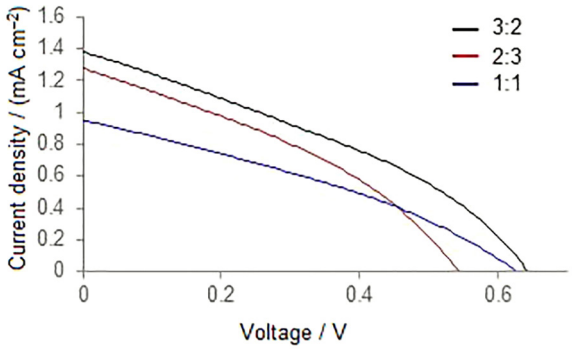

Figure 7. Photovoltaic response of 1:1, 2:3 and 3:2 **7b**:poly-(3-hexylthiophene) (P3HT) devices.

Table 3. Parameters of **7b**:poly-(3-hexylthiophene) (P3HT) photovoltaic devices

7b:P3HT	V_{OC} / V	J_{SC} / (mA cm^{-2})	FF	η / %
1:1	0.626	0.95	0.33	0.20
2:3	0.544	1.27	0.35	0.24
3:2	0.644	1.38	0.34	0.30

FF: Fill factor; J_{SC}: short-circuit current; V_{OC}: open-circuit voltage; η: power conversion efficiency.

The open-circuit voltage for the highest efficiency cell was 0.644 V, which is comparable to values observed for P3HT:PCBM devices. However, the short-circuit current densities were very low. The reduction potential of **7b** is higher than that for PCBM (−1.05 V *vs.* Ag/Ag^+ in THF).[30] In fact, the value is much closer to the second reduction of PCBM (−1.46 V). The energy level difference could account for the relatively high open-circuit voltages. Because the reduction potential is considerably higher, it is possible that a more stable P3HT state provides a pathway for recombination. The electron in the **7b**-anion could relax to a lower energy P3HT triplet state or polaron state, thus reducing overall efficiency.[31]

Alternatively, the morphology of the solar cell device could be the cause of the observed low currents. The lack of stacked domains may mean that intermolecular electron transfer is limited, which would lead to the observed low currents. Devices were fabricated using procedures optimized for PCBM devices for comparison. Efficiencies may be improved by optimizing fabrication procedures and/or active layer compositions for these functionalized corannulenes.

Conclusions

In short, a series of (phenylthio)$_n$corannulenes was synthesized and their properties investigated. There is a rough linear dependence between the HOMO-LUMO gaps and the number of substituents. This is demonstrated in the results found for both redox potentials and UV-Vis absorption data. Fabrication of a **7b**:P3HT photovoltaic device resulted in a 0.3% PCE.

Supplementary Information

Experimental procedures and photophysical spectra are available free of charge at http://jbcs.sbq.org.br. CCDC-1446812 contains the supplementary crystallographic data for this paper. The data can be obtained free of charge from The Cambridge Crystallographic Data Centre via www.ccdc.cam.ac.uk/getstructures.

Acknowledgments

We gratefully acknowledge the support of the University of Zurich, the Swiss National Science Foundation (A. S., A. B., A. L., K. K. B., J. S. S.), Robert A. Welch Foundation (endowed chair, grant #AH-0033, L. E.), US National Science Fundation (NSF), grants: DMR-1205302 (PREM Program) and CHE-1408865 (L. E., A. M.-O., D. C. B., R. W. C.), National Basic Research Program of China 2015CB856500 (K. K. B., J. S. S.), Qian Ren Scholar Program of China (K. K. B., J. S. S.), and Synergetic Innovation Center of Chemical Science and Engineering, Tianjin (K. K. B., J. S. S.).

References

1. Echegoyen, L. E.; Herranz, M. A.; Echegoyen, L. In *Encyclopedia of Electrochemistry*; Bard, A. J.; Stratmann, M.; Scholz, F.; Pickett, C. J., eds.; Wiley-VCH: Weinheim, 2007, ch. 6.2.
2. Seiders, T. J.; Baldridge, K. K.; Gleiter, R.; Siegel, J. S.; *Tetrahedron Lett.* **2000**, *41*, 4519.
3. Wu, Y.-T.; Siegel, J. S.; *Chem. Rev. (Washigton, DC, U. S.)* **2006**, *106*, 4843.
4. Niamnont, N.; Kimpitak, N.; Wongravee, K.; Rashatasakhon, P.; Baldridge, K. K.; Siegel, J. S.; Sukwattanasinitt, M.; *Chem. Commun. (Cambridge, U. K.)* **2013**, *49*, 780.
5. Lu, R.-Q.; Zhou, Y.-N.; Yan, X.-T.; Shi, K.; Zheng, Y.-Q.; Luo, M.; Wang, X.-C.; Pei, J.; Xia, H.; Zoppi, L.; Baldridge, K. K.; Siegel, J. S.; Cao, X.-Y.; *Chem. Commun. (Cambridge, U. K.)* **2015**, *51*, 1681.
6. Lu, R.-Q.; Zheng, Y.-Q.; Zhou, Y.-N.; Yan, X.-T.; Lei, T.; Shi, K.; Zhou, Y.; Pei, J.; Zoppi, L.; Baldridge, K. K.; Siegel, J. S.; Cao, X.-Y.; *J. Mater. Chem. A* **2014**, *2*, 20515.
7. Seiders, T. J.; Elliott, E. L.; Grube, G. H.; Siegel, J. S.; *J. Am. Chem. Soc.* **1999**, *121*, 7804.
8. Schmidt, B. M.; Topolinski, B.; Roesch, P.; Lentz, D.; *Chem. Commun. (Cambridge, U. K.)* **2012**, *48*, 6520; Schmidt, B. M.; Seki, S.; Topolinski, B.; Ohkubo, K.; Fukuzumi, S.; Sakurai, H.; Lentz, D.; *Angew. Chem., Int. Ed.* **2012**, *51*, 11385; Kuvychko, I. V.; Dubceac, C.; Deng, S. H. M.; Wang, X.-B.; Granovsky, A. A.; Popov, A. A.; Petrukhina, M. A.; Strauss, S. H.; Boltalina, O. V.; *Angew. Chem., Int. Ed.* **2013**, *52*, 7505.
9. Mayor, M.; Lehn, J.-M.; Fromm, K. M.; Fenske, D.; *Angew. Chem., Int. Ed.* **1997**, *36*, 2370; Mayor, M.; Lehn, J.-M.; *J. Am. Chem. Soc.* **1999**, *121*, 11231.
10. Baldridge, K. K.; Hardcastle, K. I.; Seiders, T. J.; Siegel, J. S.; *Org. Biomol. Chem.* **2010**, *8*, 53.
11. Kennedy, R. D.; Ayzner, A. L.; Wanger, D. D.; Day, C. T.; Halim, M.; Khan, S. I.; Tolbert, S. H.; Schwartz, B. J.; Rubin, Y.; *J. Am. Chem. Soc.* **2008**, *130*, 17290.
12. Valenti, G.; Bruno, C.; Rapino, S.; Fiorani, A.; Jackson, E. A.; Scott, L. T.; Paolucci, F.; Marcaccio, M.; *J. Phys. Chem. C* **2010**, *114*, 19467; Mack, J.; Vogel, P.; Jones, D.; Kaval, N.; Sutton, A.; *Org. Biomol. Chem.* **2007**, *5*, 2448.
13. Zoppi, L.; Siegel, J. S.; Baldridge, K. K.; *WIREs Comput. Mol. Sci.* **2013**, *3*, 1.
14. Zabula, A. V.; Filatov, A. S.; Spisak, S. N.; Yu, A.; Rogachev, A.; Petrukhina, M. A.; *Science (Washington, DC, U. S.)* **2011**, *333*, 1008; Eisenberg, D.; Quimby, J. M.; Jackson, E. A.; Scott, L. T.; Shenhar, R.; *Chem. Commun. (Cambridge, U. K.)* **2010**, *46*, 9010; Bauert, T.; Zoppi, L.; Koller, G.; Siegel, J. S.; Baldridge, K. K.; Ernst, K.-H.; *J. Am. Chem. Soc.* **2013**, *135*, 12857.
15. Grimme, S.; *J. Comput. Chem.* **2006**, *27*, 1787.
16. Weigend, F.; Ahlrichs, R.; *Phys. Chem. Chem. Phys.* **2005**, *7*, 3297.
17. Baldridge, K. K.; Klamt, A.; *J. Chem. Phys.* **1997**, *106*, 6622; Klamt, A.; Schürmann, G.; *J. Chem. Soc., Perkin Trans. 2 (1972-1999)* **1993**, *2*, 799.
18. Klamt, A.; Jonas, V.; Bürger, T.; Lohrenz, C. W.; *J. Phys. Chem.* **1997**, *102*, 5074.
19. Ochterski, J. W.; Petersson, G. A.; Montgomery Jr., J. A.; *J. Chem. Phys.* **1996**, *104*, 2598.
20. Hanwell, M. D.; Curtis, D. E.; Lonie, D. C.; Vandermeersch, T.; Zurek, E.; Hutchison, G. H.; *J. Cheminf.* **2012**, *4*, 17; Montgomery, J. A.; Frisch, M. J.; Ochterski, J. W.; Petersson, G. A.; *J. Chem. Phys.* **2000**, *112*, 6532.
21. Grube, G. H.; Elliott, E. L.; Steffens, R. J.; Jones, C. S.; Baldridge, K. K.; Siegel*, J. S.; *Org. Lett.* **2003**, *5*, 713.
22. Reisch, H. A.; Bratcher, M. S.; Scott, L. T.; *Org. Lett.* **2000**, *2*, 1427.
23. Scott, L. T.; *Pure Appl. Chem.* **1996**, *68*, 291.
24. Wu, Y.-T.; Maag, R.; Linden, A.; Baldridge, K. K.; Siegel, J. S.; *J. Am. Chem. Soc.* **2008**, *130*, 10729.
25. Wu, Y.-T.; Bandera, D.; Maag, R.; Linden, A.; Baldridge, K. K.; Siegel, J. S.; *J. Am. Chem. Soc.* **2008**, *130*, 10729.
26. Cremonesi, P.; Rogan, E.; Cavalieri, E.; *Chem. Res. Toxicol.* **1992**, *5*, 346.
27. Bruno, C.; Benassi, R.; Passalacqua, A.; Paolucci, F.; Fontanesi, C.; Marcaccio, M.; Jackson, E. A.; Scott, L. T.; *J. Phys. Chem. B.* **2009**, *113*, 1954.
28. Bailey, S. I.; Leung, W.-P.; *Electrochim. Acta* **1985**, *30*, 1985.
29. Kuroda, H.; Kobayashi, M.; Kinoshita, M.; Takemoto, S.; *J. Chem. Phys.* **1962**, *36*, 457.
30. Hummelen, J. C.; Knight, B. W.; LePeq, F.; Yao, J.; Wilkins, C. L.; Wudl, F.; *J. Org. Chem.* **1995**, *60*, 532.
31. Cook, S.; Furube, A.; Katoh, R.; *Energy Environ. Sci.* **2008**, *1*, 294.

Submitted: January 19, 2016
Published online: March 9, 2016